**Supporting information** for "A new route to highly structured organic glasses" by Camille Bishop, Jacob L. Thelen, Eliot Gann, Michael F. Toney, Lian Yu, Dean M. DeLongchamp, M. D. Ediger.

**SI Section 1. NEXAFS orientation and peak analysis.**

The normalized NEXAFS data for posaconazole can be described by nine Gaussian peaks and a step-edge, as shown in Figure S1.

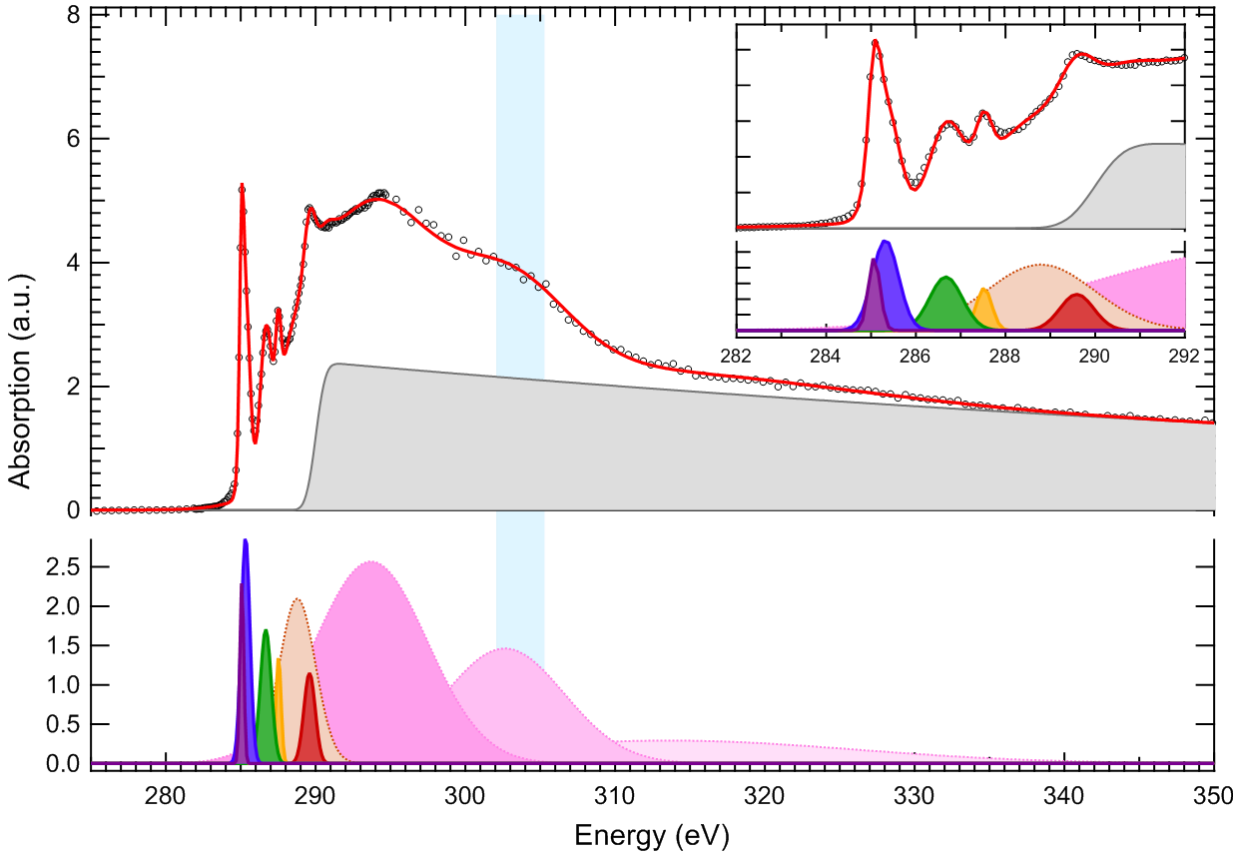


**Figure S1**. Magic-angle ($\theta_{in}$ = 55°) NEXAFS data (black circles) and fit (red curve) for posaconazole. The nine Gaussian contributions to the fit, as well as the step-edge contribution are also plotted as shaded regions for reference.

The incident-angle-dependent NEXAFS data for the liquid-cooled glass of posaconazole (deposited at 334K) were fit by adjusting only the peak heights for the Gaussian peaks shown in Figure S1. The fits were performed using the multipeak analysis in QANT (1) and are shown in Figure S2.

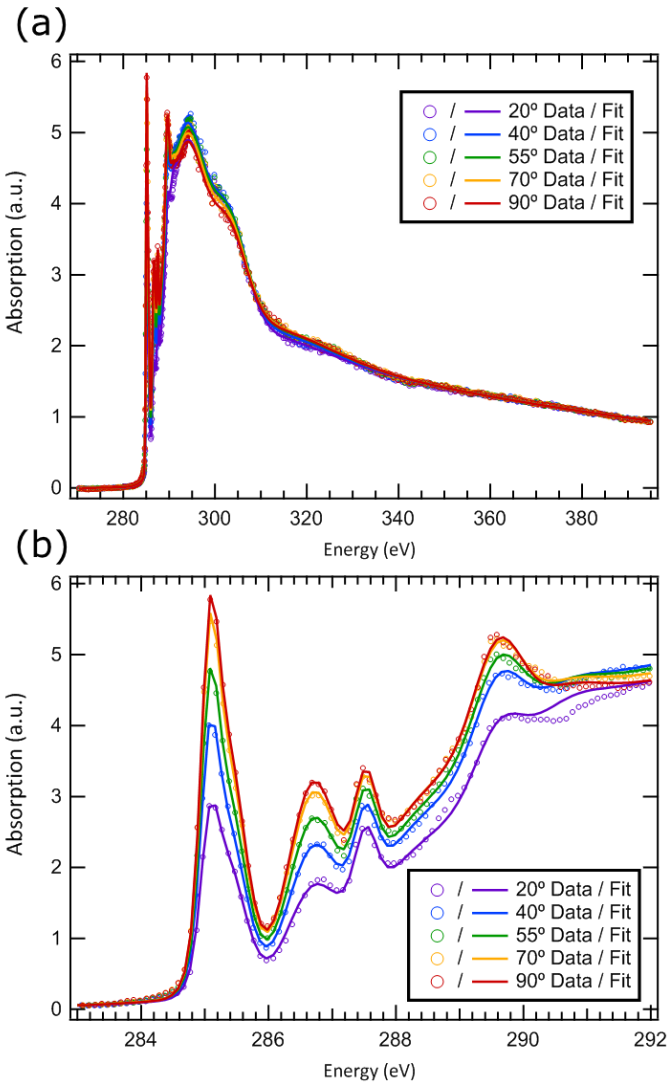


**Figure S2.** Incident-angle-dependent NEXAFS data (circles) and fits (curves) for posaconazole deposited at 334K. (a) Full range of data fitted by the Gaussian and step-edge functions shown in Figure S1, and (b) highlight of the 1s →π* resonance region.

We focus on the 5 sharpest, lowest-energy 1s→π* resonances. The integrated peak intensity as a function of incidence angle was fit to Equation S1:

$$I(\gamma,\theta) = A * \left\{\frac{2}{3}\left[1 - \frac{1}{4}(3cos^2\theta - 1)(3cos^2\gamma - 1)\right]\right\} \text{ (Equation S1)}$$

where θ is the incidence angle of the radiation, γ is the angle between the molecular long-axis and the substrate normal, and A is a normalization factor. Equation S1 is equivalent to Stöhr's plane symmetry formula 9.17a (2). The plane symmetry formula provides the correct molecular long-axis orientation because each of the 1s→π* resonances, which have vector symmetry normal to the plane of the conjugated rings (equally adopt all orientations orthogonal to the molecular long axis), effectively traces out a plane with the molecular long axis as its surface normal. Thus, the orientation of the effective plane determined by Equation S1 provides the orientation of the long axis of the molecule. A representative fit to Equation S1 from the peak centered at 286.7 eV is shown in Figure S3. The fit result indicates that on average, the long-axis is tilted ~33° from the surface normal. Each of the 1s→π* resonance peaks were fitted as shown in Figure S3 using the QANT macro (1), and the resulting long-axis orientation results are shown in Table S1.

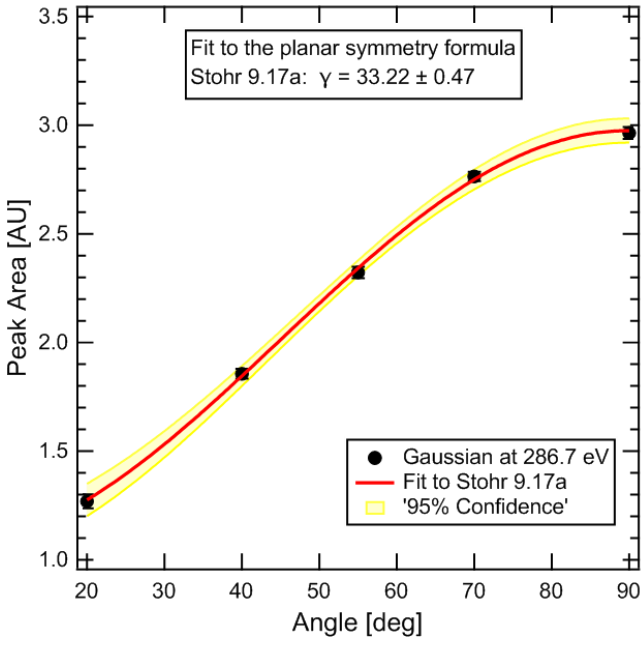


**Figure S3**. Integrated peak intensities of 1s→π* transitions centered at 286.7 eV (black circles), with fit to Equation S1 (red curve). The gold shaded band indicates the 95% confidence interval for the fit.

| Peak Position (eV) | γ - Stohr 9.17a (degrees) |
|---|---|
| 285.1 | 35.4 +/- 0.6 |
| 285.3 | 37.8 +/- 0.4 |
| 286.7 | 33.2 +/- 0.5 |
| 287.5 | 46 +/- 1 |
| 289.6 | 43.1 +/- 0.7 |

**Table S1**. Long-axis orientation results from fitting the angle-dependent peak areas to Equation S1.

In order to assign the 1s→π* resonances at 286.7 eV and 287.5 eV in the NEXAFS spectra, in Figure S4 we provide the magic-angle ($\theta_{in}$ = 55°) NEXAFS data for posaconazole and the related molecule, itraconazole. These data were collected using the NEXAFS endstation at the SST-1 beamline at NSLS-II. The data were collected in partial electron yield mode (PEY) using a channeltron detector with a -50V grid bias. The data were processed in QANT (1): the channeltron values were corrected for the incident flux using the gold mesh channel, and then the spectra were normalized to 0 prior to resonant absorption and 1 at energies well above the absorption edge. The major chemical difference between the two molecules is that itraconazole has a dichlorinated phenyl ring, while posaconazole has a difluorinated phenyl ring. The 1s →π* transition resonances for C=CCl and C=CF bonds on substituted benzene rings are expected to occur at 286.3 eV and 287.5 eV, respectively (3). The absence of a peak at 287.5 eV in the itraconazole data allows us to assign the 287.5 eV peak present in the posaconazole spectra to the fluorine-substituted carbons. This assignment is further supported by the increase in peak intensity near 286.3 eV in the itraconazole spectra, which we attribute to the 1s →π* resonance for the chlorine-substituted carbons. Thus the 286.7 eV peak in the posaconazole spectra likely contains contributions from the triazole and triazolone C=N 1s →π* resonances, as well as the C=CN and possibly C=CO 1s →π* resonances from the substituted aromatic rings in the core of the molecule.

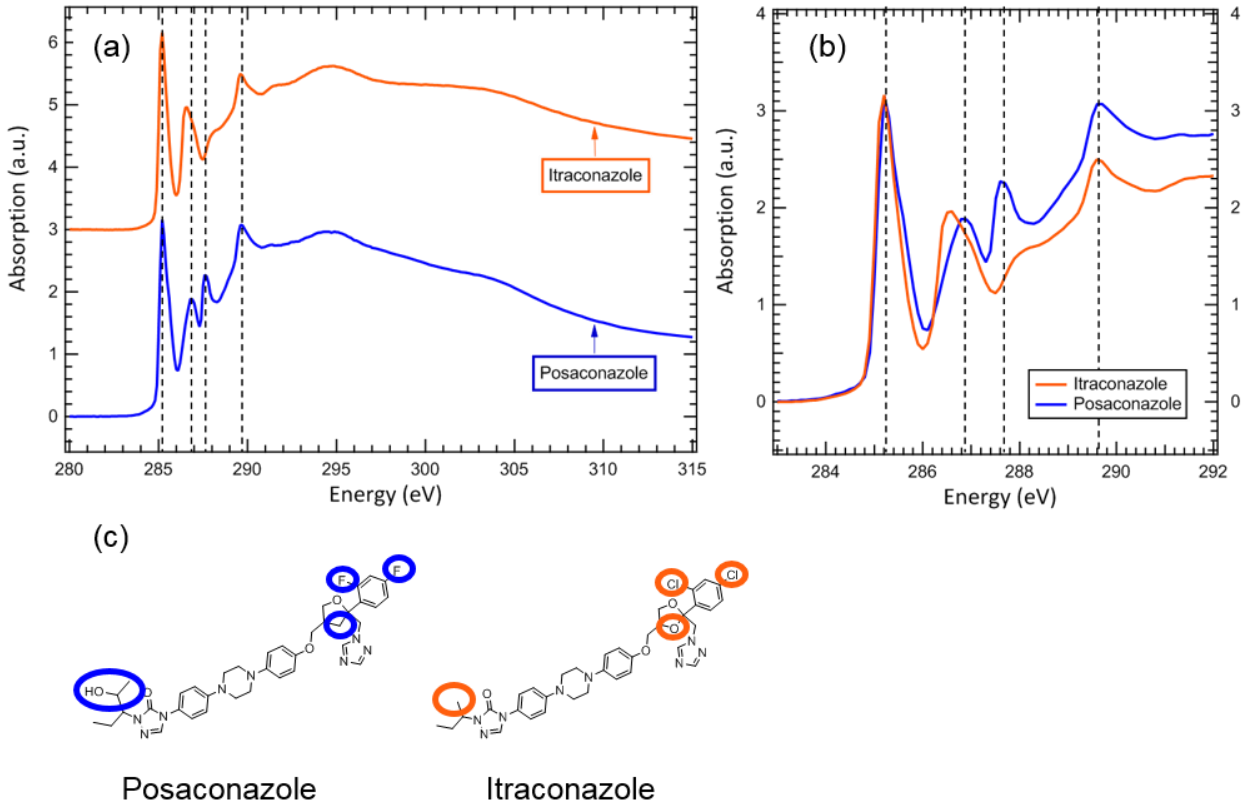


**Figure S4**. NEXAFS spectra for itraconazole and posaconazole. In (a), the spectra are offset for clarity, and in (b) the spectra are overlaid in the 1s →π* region for comparison. (c) shows the molecular structures of posaconazole and itraconazole, with differences circled.

**SI Section 2. Bulk orientation of liquid-cooled glass.**

Ellipsometry was performed on the sample used for NEXAFS at 9 points using 7 incident angles. Data between 500 and 1000 nm were fit to an anisotropic Cauchy model, in which the ordinary and extraordinary refractive indices are given, respectively, by

$$n_o = A_o + \frac{B}{\lambda^2} \text{ and } n_e = A_e + \frac{B}{\lambda^2} \quad \text{(Equation S2)}$$

Birefringence is equal to $n_e - n_o$. Over nine points, the average birefringence was 0.0006 ± 0.0008, with a minimum value of -0.0008 and a maximum value of 0.0015. These values are consistent with an isotropic film.

**SI Section 3. Bulk orientational order of vapor-deposited glass.**

We quantify the bulk orientational order to compare to the NEXAFS. We stress that the NEXAFS data may not be an exact measure of orientation at only the surface monolayer, since the probe depth of 6 nm is equal to approximately two molecular lengths. We also note that the GIWAXS order parameter does not report the molecular orientation, but rather the orientational order of anisotropic molecular packing. Therefore, the two measures of order can be compared only qualitatively.

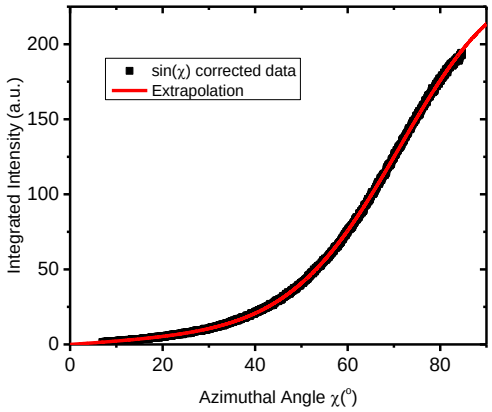


**Figure S5**. Radial integration of GIWAXS from $q$ = 1.1 to 1.7 Å$^{-1}$ of an extremely ordered glass of posaconazole deposited at 325 K and 0.02 nm s$^{-1}$.

A GIWAXS order-parameter for the scattering feature at $q \approx 1.3$ Å$^{-1}$ was calculated according to Gujral et. al. (4), with a result of -0.28. $S_{GIWAXS}$ quantifies the distribution of scattering intensity at an azimuthal angle $\chi$ (defined as 0° along $q_z$) by

$$S_{GIWAXS} = \frac{1}{2}(3\langle cos^2\chi\rangle - 1) \qquad \text{(Equation S3).}$$

$S_{GIWAXS}$ can vary between the limits of +1 and -0.5. The order parameter of -0.28 indicates a concentration of intensity from scattering of the $q \approx 1.3$ Å$^{-1}$ feature near the $q_{xy}$ direction. This concentration of scattering nearly in-plane is consistent with a picture in which mostly vertically oriented posaconazole molecules pack laterally in-plane with a nearest-neighbor distance of ~ 0.48 nm. The large width of the peak, with a coherence length of 2.9 nm as stated in the main text, is consistent with an amorphous or liquid-like packing.

**SI Section 4. Avoiding beam damage.**

To minimize beam damage, measurements were made at four different spots during annealing. Exposures lasted 30 seconds to minimize beam damage while optimizing signal-to-noise and time resolution. Before annealing, five spots were measured and found to be structurally equivalent, with 2D patterns shown in Figure S6. To quantify the orientational order, we calculate the GIWAXS order parameter (27) for each spot before and after annealing, shown in table S2. The order parameters before and after all match within error, so we combine data from different spots into one *in situ* measurement. One spot was not measured at all during annealing; after the sample was cooled, the spot's structure was isotropic. The evolution of molecular packing observed is therefore a result of the thermal treatment, and not any X-ray damage.

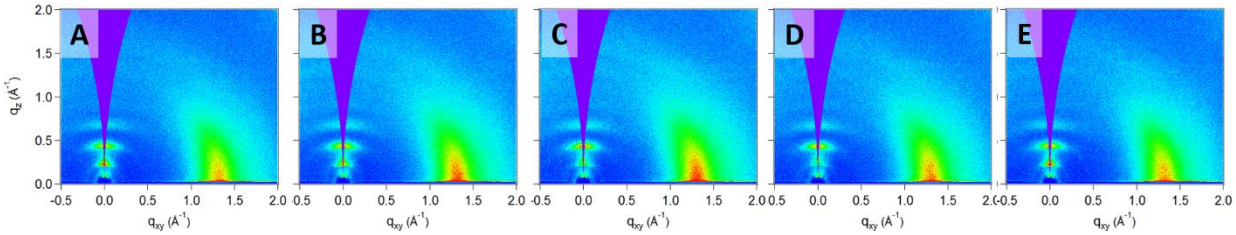


**Figure S6**. GIWAXS before annealing of five distinct spots.

| Spot | $S_{GIWAXS}$ before | $S_{GIWAXS}$ after |
|---|---|---|
| A | -0.283 | 0.006 |
| B | -0.268 | 0.007 |
| C | -0.264 | 0.004 |
| D | -0.272 | 0.004 |
| E | -0.279 | 0.005 |

**Table S2**. GIWAXS order parameter before and after annealing for all five spots.

As-deposited glasses shown in Figures 1 and 3 are not damaged by the beam, as illustrated by the following test. For a sample prepared at the same conditions as the one shown in Figure S6C, one 45-second exposure at $\theta_{in}$ = 0.14° was taken before other measurements. It then received 600 s of X-ray exposure, after which a final 45-second exposure at $\theta_{in}$ = 0.14° was taken. Within measurement error, the two 45-second exposures had identical amounts of orientational and translational order.

## References


1. Gann E, McNeill CR, Tadich A, Cowie BCC, Thomsen L (2016) Quick AS NEXAFS Tool (QANT): a program for NEXAFS loading and analysis developed at the Australian Synchrotron. *J. Synchrotron Radiat.* 23(1):374-380.
2. Stöhr J (1992) NEXAFS Spectroscopy (Springer-Verlag, Berlin) 2nd Ed.
3. Cooney RR, Urquhart SG (2004) Chemical Trends in the Near-Edge X-ray Absorption Fine Structure of Monosubstituted and Para-Bisubstituted Benzenes. *J. Phys. Chem. B* 108(47):18185-18191.
4. Gujral A, O'Hara KA, Toney MF, Chabinyc ML, Ediger MD (2015) Structural characterization of vapor-deposited glasses of an organic hole transport material with X-ray scattering. *Chem. Mater.* 27:3341-3348.